11th International Conference on Power Electronics-ECCE Asia
May 22 - 25, 2023 / ICC Jeju, Jeju, Korea

A Distribution of Relaxation Time Approach on Equivalent Circuit Model Parameterization to Analyse Li-ion Battery Degradation

E. Aguilar Boj [1], S. Azizighalehsari [1 *], P. Venugopal [1], G. Rietveld [1 2] and T. Batista Soeiro [1]
[1] Power Electronics & EMC Group, University of Twente, Enschede, The Netherlands
[2] VSL, Delft, The Netherlands
[*] E-mail: s.azizighalehsari@utwente.nl

***Abstract*—The time-varying and complex electrochemical behaviour inherent to Li-ion batteries cause a great challenge to its diagnostics and prognostics. Electrochemical impedance spectroscopy (EIS) based mapping of the impedance datasets as a function of frequency to equivalent electrical elements specific to physical/chemical characteristics is vital to validate the equivalent circuit models (ECM). Distribution of relaxation times (DRT) is a method to convert the EIS impedance spectra as a function of frequency to a distribution of time constants representing an RC network in a battery ECM. Modeling the battery with detailed consideration of EIS data is the main advantage of the DRT technique. In this work, the whole process of modeling a large amount of EIS data has been done automatically, selecting only the dominant peaks present during the entire battery ageing to increase computational efficiency. The results show that good accuracy is achieved in monitoring the degradation of a Li-ion cell and that the dispersion of the different fits is consistent throughout the data set.**

***Keywords*—Diagnostics and Prognostics, Distribution of Relaxation times (DRT), Electrochemical Impedance Spectroscopy (EIS), Equivalent Circuit Models (ECM)**

I. Introduction

Lithium-ion batteries are one the most appropriate type of energy storage to achieve decarbonization goals due to their striking specification in terms of specific power and energy, energy efficiency, response time, etc [1]. Besides all these exceptional advantages, Li-ion batteries suffer from capacity fading due to ageing. To enhance the battery's practical use and guarantee safe operation conditions, each Li-ion battery needs to be tailored with a Battery Management System (BMS) [2]. One of the main functions of the BMS is related to battery diagnostics and prognostics [3]. State of Health (SoH) is an essential parameter in battery diagnostic to show the battery's capability to store energy during the time due to the decremental capacity nature of the battery. Estimating the battery State of Charge (SoC) to avoid unexpected failure of the energy storage system is indeed one of the most critical parameters for the battery's safe operation. Additionally, having a deep understanding of the battery state can open the possibility for the battery's second-life applications that significantly impact battery longevity [4]. A detailed understanding of the battery's capacity fading mechanism/ageing facilitates the way to achieve an advanced BMS with a longer cycle life for the battery. One of the common approaches to battery SoC and SoH estimation is based on the electrical Electrical Equivalent Model (ECM). Model-based estimation methods are very dependent on the accuracy of the model parametrization and the algorithm to interpret the ageing data to a proper circuit model. It means that to have an accurate estimation, it is essential to have comprehensive data from the battery's ageing under different operation conditions and a proper model to fit the data by an appropriate algorithm.

On their counterpart, using an ECM requires deciding what form the circuit will take. This can introduce ambiguity as different ECM network configurations may have the same frequency response [5]. The error induced by a wrong ECM selection increases when analyzing an ageing data set, as the ageing processes modify the apparent Electrochemical Impedance Spectroscopy (EIS) shape, and the amount of data makes it unfeasible to hand-tune the ECM circuit for each measurement.

Classic ECM techniques required a prior deep understanding of the impedance behaviour to make the correct assumptions of how the data is behaving. Recently, thanks to the development of the Distribution of Relaxation Times (DRT) technique, it is easier to determine the RC networks relevant to the data set and see its evolution through the ageing process. The idea behind DRT is to deconvolute the measured impedance spectra to reveal the different processes that the impedance spectra are consisting of, to support the best model selection when the underlying processes behind the EIS spectra are not profoundly known. The DRT technique has been developed to analyze complex impedance spectroscopy data, and has been used to study the dynamics of chemical reactions in different fields like fuel cells [6], batteries, or PEM electrolysis [7].

Using improvements in the DRT technique made by [8], this paper proposes to include the DRT approach in the pre-processing of the EIS data into the pipeline to data-set analysis, automating the selection of an adequate ECM that can represent the current EIS shape at each measurement. At the same time, the DRT is used to select a first prediction of the ECM parameters. An important factor in achieving accurate results is the fitting algorithm used to fine-tune the parameters. Finally, a global parametrization is made to have an ECM capable of adapting to the battery's ageing processes.

Using the DRT integration method improves the accuracy in modeling the impedance value but comes at the cost of a higher computation time.

From the DRT analysis performed in the data-set used in this paper, one can extract that there are 3 main impedance processes that have a major impact, accompanied by 2 - 3 processes with minor impact. One of the proposed models that is considered a good approximation to model battery ageing processes that adapt to this shape is a 2nd-order ECM with a Warburg element, which is a good approximation to model this data set. This is in concordance with previous literature [9], [10].

The structure of the paper is presented as follows. In section II, the different steps of the proposed algorithm are introduced, from the main methodology for EIS measurements to the DRT calculation. Subsequently, the equivalent circuit model parameters are obtained with extraction and fitting of the ECM parameters for degradation prediction. Section III shows the results of applying the proposed algorithm to the selected data set. Finally, in Section IV some conclusions on the obtained results and as well as proposals for further steps to improve this research are discussed.

II. Methodology

Fig. 1 presents the main principles of the methodology algorithm in this paper, showing the three steps taken to process the impedance data in the ECM model. The model is based on the EIS measurement over a controlled ageing data set of Lithium-Ion Battery (LIB) as illustrated in Fig. 1(a). As shown in the visual representation of the processing algorithm, the paper's methodology focuses on three main stages. First, the results of the battery ageing from the EIS measurement, second the DRT analysis to deconvolute the EIS data during the whole battery ageing process, and finally, effective modeling with a proper ECM model and parametrization of the model. A similar approach has been proposed in [11]; there, the correlation between the battery ECM parameters as a function of Open Circuit Voltage (OCV) has been investigated for different SoC and temperature. The algorithm is intended to process large amounts of data.

A. Equivalent Circuit Model (ECM)

Battery ECMs are the most well-known type of experimental model for LIBs due to their limited complexity compared to other models. There are different approaches in selecting an ECM that best represents the LIB system. In [12], a model is proposed that simulates each physical layer the cell is made of; another approach is to select an ECM that only depends on the apparent shape of the EIS measurement, and finally, there are the ECM models that intend to simulate the processes in the battery that have an impedance impact. Our model follows a mix of the two last approaches. First, with the DRT analysis it was observed which processes were present in our measurements, and from those results, the most relevant processes are included in our model. Fig. 1(b) shows a sample of the database measurements after the DRT analysis.

From the DRT analysis one can extract an ECM with three impedance processes; in this case, it is decided to use a 2nd-order ECM model with an additional Warburg element. This was found to provide a good approximation to model our data set, and is in concordance with other experiences in the literature [9], [10]. The final ECM used in our study is given in Fig. 1(c) and is formed of four elements. The first component, R_0, is modeling the internal ohmic resistance of the system. Represents the value at which the impedance spectra crosses the real impedance axis. Since in our model the inductance behaviour of the battery (positive Z_{im}) is omitted, the R_0 value is the impedance measured at the highest frequency point. The second impedance component, modeled as the $R_{sei}C_{sei}$ pair, models the passivation atributed to the Solid Electrolyte Interphase (SEI) crystallization of the battery. The third component, in this model represented by the $R_{ct}C_{ct}$ pair, models the charge transfer processes observed in the battery. And the last process that can be observed in the lowest frequency measurements of the cell, the difussion processes, are modeled as the Warburg element W_d [10].

B. Electrochemical Impedance Spectroscopy (EIS)

EIS is getting more attention to be used in Li-ion battery diagnostics and prognostics as a non-destructive technique. IN EIS the complex impedance of the battery is measured

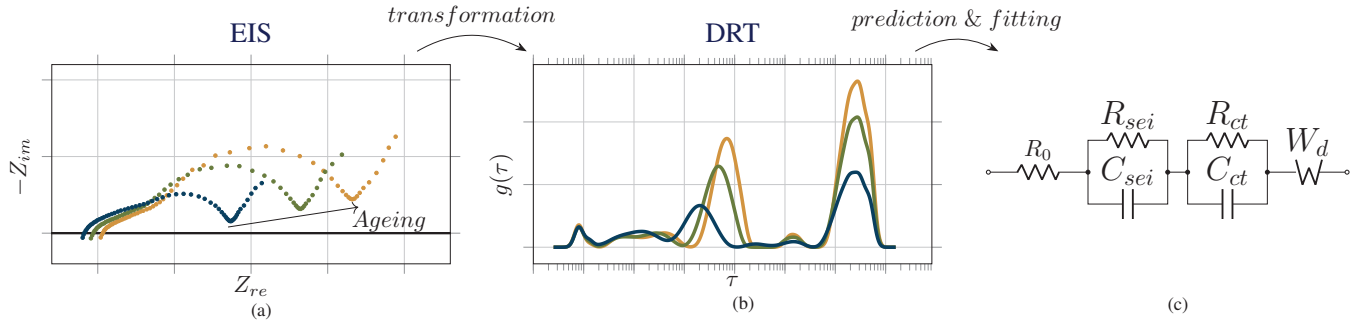

Fig. 1. Schematic overview of the steps in the proposed ECM modeling methodology. (a) Nyquist plot of an EIS measurement at different moments during the ageing process. (b) Result of processing the EIS measurements with the DRT analysis. (c) Proposed ECM derived from the DRT analysis, with parameters to be fitted from the EIS measurement data.

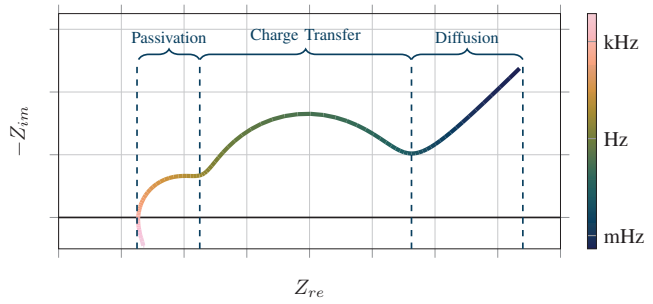

Fig. 2. Nyquist visualization of an ideal EIS measurement. As a reference, the colormap shows the frequency at which each impedance feature is happening, allowing to attribute features to different processes inside the battery.

at different frequencies. The EIS measurement is based on injecting a very small AC sweep signal within the battery and measuring the response signal in a frequency range from mHz to kHz to achieve the impedance spectra of the battery. This method helps to gain better understanding of the complex electrochemical processes that are occurring inside the battery by analyzing the impedance spectra and interpreting the data.

Previous studies, like [13], have demonstrated that some frequencies are more sensitive to changes in specific electrochemical processes governing the cell than others. Thus, by studying the changes in those regions, it is possible to grasp an idea of how the changes are affecting those processes. Fig. 2 illustrates a representation of an EIS simulation of an ideal battery, where the different processes that become manifest in the impedance are shown, and an idea of the frequency ranges at which these take place is visualized in the color map. The semi-circle observed in the high-frequency range is primarily influenced by the film's resistance and its accompanying capacitance. The arc in the medium-frequency range is caused by the charge-transfer resistance and the capacitance of the double layer. The slope at the low-frequency end is a result of the diffusion impedance [14].

From the EIS measurement, there are two parameters that can be extracted directly, which will be used later with the DRT values to fit the ECM values. R_0, the ohmic resistance of the system, is extracted from the Z value at the intersection of the Nyquist plot with the real axis at a higher frequency and the R_{pol} that is inferred using a variation of the method explained in [15]. R_{pol}, the polarization resistance, is the Z_{re} difference between the ohmic resistance of the system and the highest resistance of the system. Usually is the second crossing of the Z_{re} axis; in LIBs, due to the Constant-Phase Element (CPE) behaviour, this second crossing never occurs and is estimated with the Z_{re} measured at the lowest frequency measured.

In this paper, we sequenced the data set generated by the Cambridge university for the publication [16]. This data set has been selected because, compared with other available EIS repositories, data has enough resolution to extract features, up to 10 points per decade, ageing has been done at different temperatures, and EIS measurements have been performed at each cycle of the battery.

C. Distribution of Relaxation Times (DRT)

This paper uses the DRT analysis developed in [8]. The benefit of DRT analysis is that it allaws the deconvolution of the impedance spectra into the different processes that are present within the measurement. The EIS measurement is fitted against the DRT model

$$Z(\omega) = R_0 + \int_0^0 \frac{g(\tau)}{1 + j\omega\tau} d\tau \tag{1}$$

Where R_0 is the ohmic resistance of the system, the same shown in the section II-A, and the $g(\tau)$ is a function that represents the time relaxation of the system; showing the relevance at each point of the time domain of the infinite sum of parallel R-C.

The peaks of the function can be mapped to discrete RC networks, proposed in suitable ECM. To choose the approximation that represents the best model, it is essential to know the application for which the model is designed. In this work, as it can be seen in Fig. 4 one has a system with an R_0 and 3 RC principal components and 2 - 3 (depending on the ageing process) less prominent peaks. For the model, a double RC and a Warburg element are considered sufficient and a good balance between accuracy and computational time to produce a result.

To convert the the DRT result into an ECM, a discreet simplification of the Eq. 1 presented before is uses. Making it possible possible to map the DRT peaks to the ECM components.

$$Z(\omega) = R_0 + R_{pol} \sum_{k=0}^{n} \frac{G(\tau_k)}{1 + j\omega\tau_k} \tag{2}$$

Being $\sum_{k=0}^{n} G(\tau_k) = 1$, the normalized version of $g(\tau)$.

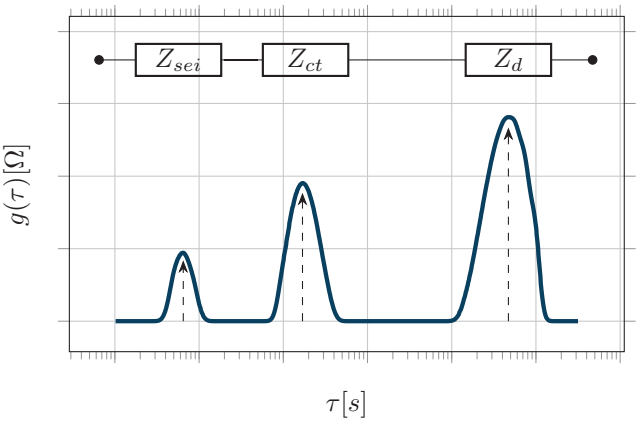

Fig. 3. DRT analysis of an ideal EIS measurement (solid line) giving the $g(\tau)$ values. The arrows mark the point where the main impedance characteristics are located and the circuit above each peak is derived from the DRT shape. The exact shape of the ECM circuit will vary depending on the studied sample; for LIB, it is common to model each impedance element using R-C or R-CPE pairs respectively.

Even though one of the benefits introduced by the DRT is giving a model-free characterization of impedance spectra this information should be analyzed due to the fact that the data obtained is sensitive to the EIS quality and the tune of some DRT parameters [17]. The DRT analysis deconvolute the impedance data and re-interprets it into $g(\tau)$ values, giving a better understanding of how relevant is every RC-element on the ECM.

In the data presented in this paper, after the DRT analysis there is a shape with three main peaks, as it is represented in the Fig. 3. Those peaks can be correlated to the processes experienced by the battery that was visualized before in Fig. 2 and simplifying the ECM selection. At the same time, discretizing the impedance spectra make it simpler to study the changes produced by the ageing at each relevant process.

In some papers like [11], [18] after performing the DRT analysis an RC value is mapped at every peak. This gives a great accuracy, but applying this technique to a whole data set introduces problems. False peaks may occur, as stated in [17], making the model inconsistent through the ageing and difficulties within the task of tracking their differences. At the same time, choosing proper ECM needs an assumption of how the system behaves. The proposed method to convert the DRT values into an ECM requires taking into account the more prominent peaks that are present in all of the data sets.

Finally, a fine adjustment to the values pre-calculated with the DRT method is done. This is to minimize the inaccuracies introduced by the R_{pol} estimation and to correct the curve for the omitted features. As stated in [19], the data is fitted with the Least Squares Fit (LQF) algorithm.

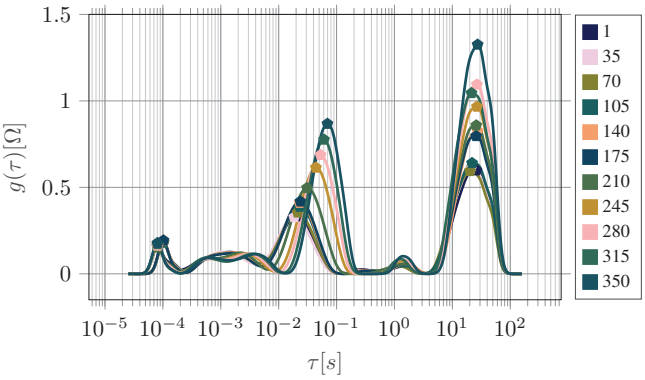

Fig. 4. Distribution of relaxation times at different cycle numbers of the Li-ion cell. Each point in the figure marks the maximum of the selected impedance features, relevant for the fitting algorithm.

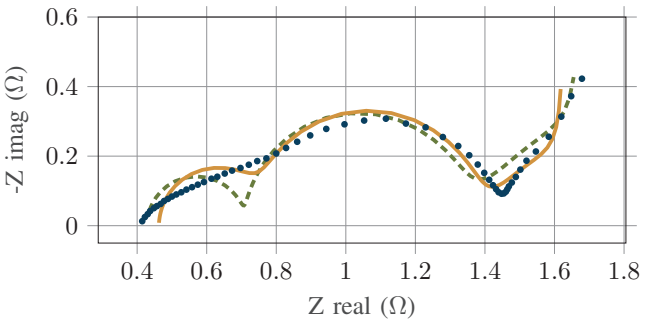

Fig. 5. Nyquist plot of cell 1 at 25 ºC on cycle 120. Comparison between the measured impedance data (blue dots) and ECM model prediction, with the parameters directly extracted from the DRT (green dashed line) and after LQF adjustment (yellow line).

III. Results

Ageing of the battery and its contribution to the model features of the cell has been visualized in Fig. 4. The distribution of the relaxation time shows that two time constants related to the RC processes drift through the battery's ageing. First time-constant related to the RC behaviour remains almost fixed through the whole ageing of the battery. There are other 2 RC characteristics present in the data, close to τ values of 10^{-3} and 10^{0}, that their g value remains relatively constant through the ageing process, but their prominence is minor. For our application, a conscious decision has been made to omit features from our ECM, which are minimal contributors to increasing the accuracy while decreasing the computational efficiency.

To assure that model tracks the same features through the ageing, the g values are passed through an algorithm that tracks the selected points across the ageing.

Once the dominant peak points are selected, the $g(\tau)$ values are converted to the RC network. In Fig. 5 a Nyquist plot of one of the EIS measurements of the data set has been shown. The estimation is directly extracted from the DRT values and the better approximation is deduced with the LQF algorithm. One of the problems of the LQF is the initial values given to the algorithm, as the accuracy of them influences the accuracy of the final fit. The DRT approach optimizes this step, feeding the algorithm with a good first approximation.

The residuals of the impedance have been visualized for the proposed modeling technique in Fig. 6 and, one can inhere the residuals of the whole processes data, by calculating $Z_{calc}(\omega) - Z_{meas}(\omega)/Z_{meas}(\omega)$. The error at each frequency point is consistent through the ageing process, thus dependent on the ECM chosen. At the same time, the accuracy through the studied frequency falls inside the accuracy predicted through the DRT to selected ECM. Table I shows the fit values of the different ECM components of Fig. 1(c) for the selected cycles of Fig. 4.

Compared to the process explained in this paper with a more traditional approach, we can see the average error residuals displayed in Fig. 6(a) and Fig. 6(b). Both graphs represent the same data; in the upper sub-figure, the data has been processed using the results of the DRT analysis to feed the fitting algorithm with a good first guess of the values. The second sub-figure represents the same section of the data-set but without using the values of the DRT analysis. Comparing both results, in lower frequencies, they have similar fitting accuracy, but over the boundary of 1Hz the results given by the process that includes the DRT have less dispersion in the

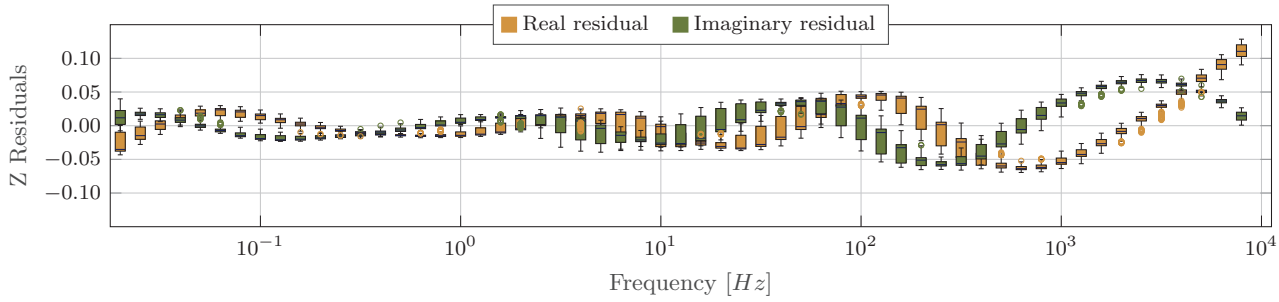

(a) Fitting data with DRT input

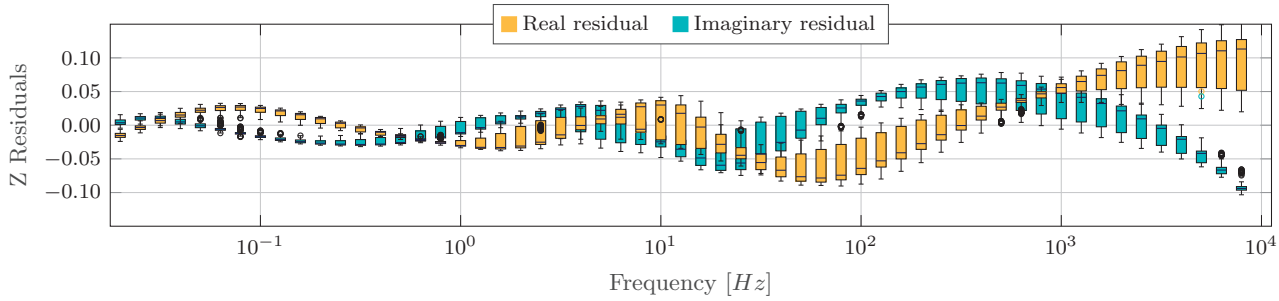

(b) Fitting data without DRT input

Fig. 6. Fit residual values of the real and imaginary parts of the impedance as a function of frequency. The boxes represent the values within the first and third quartile of all the measurements taken at that frequency point, whereas the dark blue bar represents the median of the data. (a) gives the result after applying the DRT approach explained in this paper, whereas (b) is the result after the same fitting process but with omitting the DRT approach.

TABLE I
VALUES OF THE ECM PARAMETERS FITTED WITH THE DRT METHOD AS A FUNCTION OF AGEING (CELL CYCLING).

Cycle Nr	R_0 [Ω]	R_{sei} [Ω]	C_{sei} $[mF]$	R_{ct} [Ω]	C_{ct} $[mF]$	W_d [Ω]	W_d $[s]$
1	0.463	0.297	1.83	0.519	30.0	0.821	27.28
35	0.426	0.280	1.94	0.513	28.7	1.89	148.2
70	0.433	0.284	2.09	0.546	30.0	1.89	142.3
105	0.446	0.289	2.23	0.581	30.6	1.97	147.3
140	0.450	0.290	2.18	0.599	30.2	0.798	18.15
175	0.462	0.282	2.19	0.605	30.4	0.834	19.00
210	0.500	0.286	2.34	0.692	35.7	0.907	19.80
245	0.520	0.289	2.77	0.818	22.9	1.05	20.23
280	0.533	0.298	2.98	0.897	46.3	1.12	19.24
315	0.600	0.289	3.07	0.969	49.3	1.27	22.34
350	0.598	0.296	3.27	1.06	52.4	1.24	18.53

results, as their Inter-Quartile Range (IQR) is smaller. And, in a small order of magnitude, the average error presented in the DRT approach is more minor than not using this computation.

This difference is caused by the high sensitivity that the LQF algorithm has to the initial values to produce a better result. When processing a reduced amount of data is feasible to hand pick good starting values for all the measurements, but when dealing with a large amount of data an algorithm that can extract these initial values is necessary.

Without entering into the chemical reactions occurring in the cell, different degradation processes that affect the battery can be grouped into two main groups, the processes that end up reducing the maximum capacity of the battery and the processes that increase the impedance of the battery. The DRT method proposed in this paper is intended to analyze the impedance degradation processes. In Fig. 7, the ageing process of the Z_{ct} and the change in their capacitance and resistance can be observed. The data shown correspond to 7 batteries in the data set aged at different temperatures, marked by the first number in their name (25º,35º,45º).

From the data present in the data set, it can be extrapolated that the ageing process in the charge Transfer part of the battery is influenced by the temperature only on the resistivity part.

In the sub Fig. 7(a), the slope at which the resistance increase is highly influenced by the temperature; having clearly delimited the different temperatures present in the data set.

From the data present sub Fig. 7(b), the rate at which the capacity is degraded does not appear to be influenced by the temperature difference among the cells. They appear to have a similar degradation rate, with small variations that could be explained by the initial differences of the cells.

The data set used for this analysis had a high disparity between the cells at their beginning of life, with some cells having worse impedance characteristics at the start of the test than others at the end. To compensate this disparity and show

only the change produced by the ageing on the test the graphs in Fig. 7 had been normalized to the value of their beginning of life; showing the relative ageing from their starting conditions.

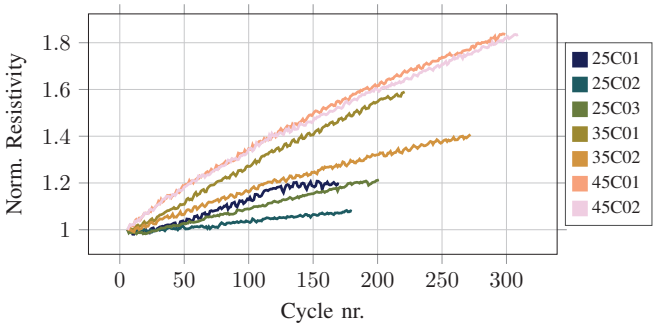

(a) Normalized R_{ct}

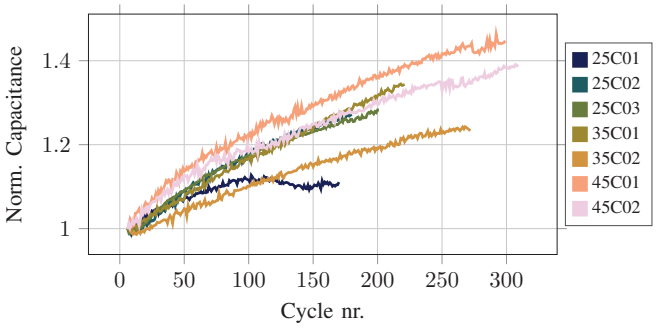

(b) Normalized C_{ct}

Fig. 7. Charge transfer impedance drift, divided into resistance (a) and capacitance (b). It can be seen that the resistance component R_{ct} correlates with temperature, whereas the capacitance C_{ct} increase is very similar for different temperatures.

IV. Conclusion

In this paper, an automated DRT analysis approach has been developed aiming to facilitate the ECM modeling process of an ageing lithium-ion battery for a large amount of EIS data. ECM modeling of a battery is a powerful approach to interprete data from EIS measurements, where the different model elements in the ECM describe the various physical and chemical processes occurring within the battery. It appears that the EIS information is rich enough to discern the different elements of the cell performance modeled by the main ECM elements and that the DRT analysis approach helps to increase the accuracy of the modeling. The result achieved with the new approach has been compared to a modeling approach without applying the DRT step.

DRT calculation is an ill-posed problem, and due to the heavy computing power it requires, it is necessary to do some pre-processing of the data. The first step is to prepare the data in the standard EIS format and select the proper frequency range with the most valuable information regarding the battery electrochemical process. Subsequently, the data are converted from the frequency domain into a distribution of time constants and interpreted into $g(\tau)$, in order to parameterize the ECM elements.

After applying the proposed analysis technique, it has been found that this approach can also reduce the amount of lost information from the EIS measurement, calculating the ECM parameters more consistently and thus decreasing the IQR bands of the errors.

Especially when the model is not approximating the real situation well, fitting algorithms are sensitive to their starting value to find the suitable minima of the function to parameterize. This is caused by a flaw of the impedance simulation through ECM, that different combination of component values may produce the same impedance frequency behaviour. The DRT analysis isolates the different impedance processes that occur in the battery, allowing one to choose the ECM values linked only to one of these processes. This opens the possibility to study the change of the battery characteristics by tracing the changes of each parameter of the ECM.

After having a good fit of the parameters, it is possible to analyze the changes produced by the ageing on the fitted parameters. As shown in the results, this ageing data set has a high correlation between the resistance of the charge transfer processes with the temperature at which the battery cell is operating. In our future work, we will use the DRT approach for ECM parametrization presented in this paper for further evaluation of the ageing behaviour of a series of LIB cells under different conditions.

Acknowledgements

References

[1] M. Knipper, N. Ó Brolcháin, A. De Shryver, *et al.*, *State of the Art Report on Storage Technologies, Opportunities and Trends*, English, P. Mouratidis, Ed. Interreg North-West Europe, May 2021.

[2] R. Eskandari, P. Venugopal, and G. Rietveld, "Advanced battery management systems with integrated battery electronics," in *2022 IEEE 20th International Power Electronics and Motion Control Conference (PEMC)*, 2022, pp. 55–61. DOI: 10.1109/PEMC51159.2022.9962868.

[3] S. Azizighalehsari, J. Popovic, P. Venugopal, and B. Ferreira, "A review of lithium-ion batteries diagnostics and prognostics challenges," in *IECON 2021 – 47th Annual Conference of the IEEE Industrial Electronics Society*, 2021, pp. 1–6. DOI: 10.1109/IECON48115.2021.9589204.

[4] S. Azizighalehsari, P. Venugopal, D. P. Singh, and G. Rietveld, "Performance evaluation of retired lithium-ion batteries for echelon utilization," in *IECON 2022–48th Annual Conference of the IEEE Industrial Electronics Society*, IEEE, 2022, pp. 1–6.

[5] J. R. Macdonald, "Impedance spectroscopy," *Annals of Biomedical Engineering*, vol. 20, no. 3, pp. 289–305, May 1992, ISSN: 1573-9686. DOI: 10.1007/BF02368532. [Online]. Available: https://doi.org/10.1007/BF02368532.

[6] H. Schichlein, A. C. Müller, M. Voigts, A. Krügel, and E. Ivers-Tiffée, "Deconvolution of electrochemical impedance spectra for the identification of electrode reaction mechanisms in solid oxide fuel cells," *Journal of Applied Electrochemistry*, vol. 32, no. 8, pp. 875–882, Aug. 2002, ISSN: 1572-8838. DOI: 10.1023/A:1020599525160. [Online]. Available: https://doi.org/10.1023/A:1020599525160.

[7] Y. Li, Y. Jiang, J. Dang, *et al.*, "Application of distribution of relaxation times method in polymer electrolyte membrane water electrolyzer," *Chemical Engineering Journal*, vol. 451, p. 138 327, 2023, ISSN: 1385-8947. DOI: https://doi.org/10.1016/j.cej.2022.138327. [Online]. Available: https://www.sciencedirect.com/science/article/pii/S1385894722038104.

[8] T. H. Wan, M. Saccoccio, C. Chen, and F. Ciucci, "Influence of the discretization methods on the distribution of relaxation times deconvolution: Implementing radial basis functions with drttools," *Electrochimica Acta*, vol. 184, pp. 483–499, 2015, ISSN: 0013-4686. DOI: https://doi.org/10.1016/j.electacta.2015.09.097. [Online]. Available: https://www.sciencedirect.com/science/article/pii/S0013468615305090.

[9] U. Westerhoff, K. Kurbach, F. Lienesch, and M. Kurrat, "Analysis of lithium-ion battery models based on electrochemical impedance spectroscopy," *Energy Technology*, vol. 4, no. 12, pp. 1620–1630, 2016. DOI: https://doi.org/10.1002/ente.201600154. eprint: https://onlinelibrary.wiley.com/doi/pdf/10.1002/ente.201600154. [Online]. Available: https://onlinelibrary.wiley.com/doi/abs/10.1002/ente.201600154.

[10] C. Chang, S. Wang, C. Tao, J. Jiang, Y. Jiang, and L. Wang, "An improvement of equivalent circuit model for state of health estimation of lithium-ion batteries based on mid-frequency and low-frequency electrochemical impedance spectroscopy," *Measurement*, vol. 202, p. 111 795, 2022, ISSN: 0263-2241. DOI: https://doi.org/10.1016/j.measurement.2022.111795. [Online]. Available: https://www.sciencedirect.com/science/article/pii/S0263224122009976.

[11] P. Iurilli, C. Brivio, R. E. Carrillo, and V. Wood, "Eis2mod: A drt-based modeling framework for li-ion cells," *IEEE Transactions on Industry Applications*, vol. 58, no. 2, pp. 1429–1439, 2022. DOI: 10.1109/TIA.2021.3134946.

[12] U. Westerhoff, K. Kurbach, F. Lienesch, and M. Kurrat, "Analysis of lithium-ion battery models based on electrochemical impedance spectroscopy," *Energy Technology*, vol. 4, no. 12, pp. 1620–1630, 2016. DOI: https://doi.org/10.1002/ente.201600154. eprint: https://onlinelibrary.wiley.com/doi/pdf/10.1002/ente.201600154. [Online]. Available: https://onlinelibrary.wiley.com/doi/abs/10.1002/ente.201600154.

[13] J.-H. Lee and W. Choi, "Novel state-of-charge estimation method for lithium polymer batteries using electrochemical impedance spectroscopy," *Journal of Power Electronics*, vol. 11, no. 2, pp. 237–243, Mar. 2011. DOI: https://doi.org/10.6113/JPE.2011.11.2.237. [Online]. Available: http://koreascience.or.kr/article/JAKO201117148820186.page.

[14] X.-Z. Yuan, C. Song, H. Wang, and J. Zhang, "Electrochemical impedance spectroscopy in pem fuel cells: Fundamentals and applications," 2010.

[15] F. Mansfeld and W. J. Lorenz, "Determination of the polarization resistance with ac impedance measurements," *Proc. - Electrochem. Soc.; (United States)*, vol. 81-82, Jan. 1981. [Online]. Available: https://www.osti.gov/biblio/7044355.

[16] Y. Zhang, Q. Tang, Y. Zhang, J. Wang, U. Stimming, and A. A. Lee, "Identifying degradation patterns of lithium ion batteries from impedance spectroscopy using machine learning," *Nature Communications*, vol. 11, no. 1, p. 1706, Apr. 2020, ISSN: 2041-1723. DOI: 10.1038/s41467-020-15235-7.

[17] M. Hahn, S. Schindler, L.-C. Triebs, and M. A. Danzer, "Optimized process parameters for a reproducible distribution of relaxation times analysis of electrochemical systems," *Batteries*, vol. 5, no. 2, 2019, ISSN: 2313-0105. DOI: 10.3390/batteries5020043. [Online]. Available: https://www.mdpi.com/2313-0105/5/2/43.

[18] J. Xia, C. Wang, X. Wang, L. Bi, and Y. Zhang, "A perspective on drt applications for the analysis of solid oxide cell electrodes," *Electrochimica Acta*, vol. 349, p. 136 328, 2020, ISSN: 0013-4686. DOI: https://doi.org/10.1016/j.electacta.2020.136328. [Online]. Available: https://www.sciencedirect.com/science/article/pii/S0013468620307209.

[19] M. D. Murbach, B. Gerwe, N. Dawson-Elli, and L.-k. Tsui, "Impedance.py: A python package for electrochemical impedance analysis," *Journal of Open Source Software*, vol. 5, no. 52, p. 2349, 2020. DOI: 10.21105/joss.02349. [Online]. Available: https://doi.org/10.21105/joss.02349.